Am J Transl Res 2019;11(10):6475-6486
www.ajtr.org /ISSN:1943-8141/AJTR0102079

Original Article

miR-625-3p promotes migration and invasion and reduces apoptosis of clear cell renal cell carcinoma

Liwen Zhao[1*], Kaihao Liu[1*], Xiang Pan[1], Jing Quan[1], Liang Zhou[2], Zuwei Li[3], Canbin Lin[3], Jinling Xu[1], Weijie Xu[1], Xin Guan[1], Hang Li[1], Liangchao Ni[1], Yaoting Gui[1], Yongqing Lai[1]

[1]*Guangdong and Shenzhen Key Laboratory of Male Reproductive Medicine and Genetics, Peking University Shenzhen Hospital, Clinical College of Anhui Medical University, Shenzhen 518036, Guangdong, P. R. China;* [2]*Guangzhou Medical University, Guangzhou 511436, Guangdong, P. R. China;* [3]*Shantou University Medical College, Shantou 515041, Guangdong, P. R. China.* [*]*Equal contributors.*

Received May 18, 2019; Accepted September 10, 2019; Epub October 15, 2019; Published October 30, 2019

Abstract: Clear cell renal cell carcinoma (ccRCC) is a common malignancy, yet, the mechanisms underlying tumorigenesis remain unclear. Several miRNAs have been implicated in the development of RCC previously via regulation of target gene expression. As miR-625-3p has recently been identified to play a role in development of other malignancies and is reportedly upregulated in ccRCC, we sought to investigate the role of this miRNA in the progression of ccRCC. Analysis of 30 paired fresh ccRCC tissues and adjacent normal renal tissues revealed that the expression of miR-625-3p was increased in ccRCC tissues compared to normal tissues. Subsequently, in 136 formalin-fixed paraffin-embedded ccRCC tissues, the increased miR-625-3p expression was correlated with poor prognosis for ccRCC patients. The diagnostic value of miR-625-3p was identified in 50 ccRCC patients and 74 healthy controls by ROC curve. miR-625-3p was decreased in serum of ccRCC patients compared to healthy individuals. miR-625-3p could serve as a promising serum biomarker for yielding an area under the receiver operating characteristic curve of 0.792 with 70.3% sensitivity and 80.0% specificity in discriminating ccRCC from healthy individuals. Using in vitro functional assays, we found that overexpression of miR-625-3p promoted migration and invasion of ccRCC cells but reduced ccRCC cell apoptosis. Inhibition of miR-625-3p, on the other hand, exerted the opposite effects. Bioinformatic analyses indicated that predicted gene targets of miR-625-3p are correlated with lower overall survival of ccRCC patients. Together, these findings demonstrate that miR-625-3p promotes ccRCC migration and invasion and reduces apoptosis, providing a prognostic marker for survival and a potential diagnostic and therapeutic target against ccRCC.

Keywords: Renal cell carcinoma, miR-625-3p, progression, prognosis, diagnosis, biomarker

Introduction

Renal cell carcinoma (RCC) is the 9th most common cancer in men and the 14th most common cancer in women worldwide, accounting for approximately 3.77% of all new malignancy diagnoses in the United States [1-3]. Clear cell renal cell carcinoma (ccRCC) is the most common subtype of RCC [4]. Currently, surgery remains the only potentially curative approach for localized and locally advanced ccRCC [5]. Recently, multiple adjuvant treatments, such as targeted therapy and immunotherapy, have been approved based on significant responses in patients with advanced RCC. Despite these advances, essential questions regarding biomarkers of efficacy, patient selection, and the optimal combination and sequencing of reagents remain [6]. The prognosis of ccRCC is closely related to the stage of cancer. According to the American Joint Commission on Cancer (AJCC) Cancer Staging Manual, patients with stage I disease have a 5-year recurrence free-survival of more than 92%; however, the rate is less than 60% for those patients with stage II and III disease [6]. Furthermore, there are no available guidelines for screening ccRCC [7]. Thus, new therapeutic targets and screening approaches are urgently needed.

microRNAs (miRNAs) are a cluster of small noncoding RNAs with a length of 20-24 nucleo-

Table 1. Patients Characteristics

Characteristics	Number of cases
Mean age range (years)	43 (31-76)
Sexual distinction	
Male	17
Female	13
Tumor stage	
T1	17
T2	6
T3+T4	7
Fuhrman grade	
I	14
II	8
III	7
IV	1
AJCC clinical stages	
I	15
II	5
III+IV	10

pT, primary tumor; AJCC, American Joint Committee on Cancer.

tides, and these RNAs regulate target gene expression by binding to the 3'-UTR of mRNA [8]. Accumulating evidence indicates that miRNAs are involved in several tumorigenesis processes, including angiogenesis [9], proliferation [10], apoptosis [11], metastasis [12], invasion, and drug-resistance [13]. Previous studies reported that many miRNAs, including miR-141 [14], miR-532-5p [15], miR-206 [16], miR-182-5p [17], and miR-629 [18], are aberrantly expressed in RCC and play crucial roles in the development of this malignancy. Moreover, miR-625-3p was found to act as a tumor inducer or suppressor in multiple human malignancies [19-21], and The Cancer Genome Atlas (TCGA) database indicates that miR-625-3p is upregulated in ccRCC. The role of this miRNA in the development of ccRCC, however, remains unknown.

In the present study, we examined the role of miR-625-3p in ccRCC. We found that miR-625-3p expression was upregulated in ccRCC tissues and was correlated with poor prognosis of ccRCC patients. And miR-625-3p was found to be down-regulated in serum of ccRCC patients, which could discriminate ccRCC patients from healthy individuals. In addition, miR-625-3p promoted the migration and invasion of ccRCC but suppressed the apoptosis of ccRCC cells in vitro. Thus, our study suggested that miR-625-3p serve as a potential diagnostic, prognostic biomarker and a potential therapeutic target against ccRCC.

Materials and methods

TCGA dataset analysis

The expression level of miR-625-3p in ccRCC tissues was analyzed using the open-source platform starBase v3.0 (http://starbase.sysu.edu.cn/panMirDiffExp.php). Kaplan-Meier survival curves were generated using OncoLnc (http://www.oncolnc.org/) in order to investigate the relationships between miR-625-3p expression and overall survival of ccRCC patients.

Patients and sample collection

The ccRCC specimens and adjacent normal renal tissues were obtained from 30 patients who underwent surgery at Peking University Shenzhen Hospital from January 2012 to November 2015. All tissues were stored in liquid nitrogen until RNA isolation. Patients' characteristics are summarized in **Table 1**. A total of 136 formalin-fixed paraffin-embedded (FFPE) ccRCC tissues were obtained from the department of pathology at Peking University Shenzhen Hospital from February 2001 to January 2010. The characteristics of these patients are included in **Table 2**. Serum samples were obtained from 50 patients who underwent surgery between 2017 and 2019 at the Department of Urology at Peking University Shenzhen Hospital. All serum samples were collected before surgery. In addition serum samples from 74 healthy controls (HCs) were obtained. After centrifugation (3,000 rpm, 10 min) serum was separated and stored in cryotubes at -80°C. The clinicopathological parameters are shown in **Table 3**. Written informed consent was also obtained from all patients, and the study was approved by the Ethics Committee of Peking University Shenzhen Hospital.

Cell lines and cell culture

The human ccRCC cell lines Caki-1, Caki-2, 786-O, and ACHN and the human normal renal tubular epithelial cell line HK-2 were obtained from ATCC and preserved in The Guangdong

Table 2. Association between miR-625-3p Status[1] and Clinicopathologic Variables in FFPE[2] Clear-Cell Renal Cell Carcinoma Samples

Variable	Total	No. of patients (%)		*P*-value
		High	Low	
Gender				
Male	87	45 (51.7)	42 (48.3)	0.592[3]
Female	49	23 (46.9)	26 (53.1)	
Age (Years)				
≤60	70	39 (55.7)	31 (44.3)	0.170[3]
>60	66	29 (43.9)	37 (56.1)	
Tumor size (cm)				
≤4.0	62	34 (54.8)	28 (45.2)	0.302[3]
>4.0	74	34 (45.9)	40 (54.1)	
TNM stage				
I+II	99	43 (43.4)	56 (56.6)	0.012[3]
III+IV	37	25 (67.6)	12 (32.4)	

[1]cut-off point: median; [2]FFPE, Formaldehyde-fixed-paraffin-embedded; [3]Calculated with Pearson Chi-square test.

Table 3. Clinicopathological parameters of the patients providing serum

	Serum samples	
	ccRCC (n=50)	Healthy control (HC, n=74)
Sex		
Male	35	34
Female	15	40
Age (years)		
Mean	49.5	54.3
Range	24-79	35-91
Pathological stage		
pT1	43	-
pT2	6	-
pT3	1	-
pT4	0	-
Lymph nodes metastasis	0	-
Distant metastasis	0	-

and Shenzhen Key Laboratory of Male Reproductive Medicine and Genetics (Peking University). HK-2 cells were cultured in keratinocyte serum-free medium (ScienCell Research Laboratories, Inc., Carlsbad, CA, USA) supplemented with 1% keratinocyte growth supplement (ScienCell Research Laboratories, Inc.) and 1% antibiotics (100 μl/ml penicillin and 100 mg/ml streptomycin sulfates). ACHN cells were cultured in DMEM (Gibco; Thermo Fisher Scientific, Inc., Waltham, MA, USA) supplemented with 10% fetal bovine serum (FBS, Gibco; Thermo Fisher Scientific, Inc.) and 1% antibiotics. 769-P and 786-O cells were cultured in RPMI-1640 supplemented with 10% FBS and 1% antibiotics. Caki-1 and Caki-2 cells were cultured in McCoy's 5a (Gibco; Thermo Fisher Scientific, Inc.) supplemented with 10% FBS and 1% antibiotics. All cells were maintained at 37°C in a humidified atmosphere of 5% CO_2.

Quantitative real-time PCR (qRT-PCR)

Total RNA was isolated from ccRCC tissues, adjacent normal renal tissues, and cultured cells using Trizol reagent (Invitrogen, Waltham, MA, USA) and purified using miRNeasy mini kit (Qiagen GmbH, Hilden, Germany) according to the protocols supplied by the manufacturer. Total RNA of FFPE tissue was extracted using miRNeasy FFPE kit (Qiagen GmbH) according to the manufacturer's protocol. Total RNA was isolated from 200 μl serum by using the miRNeasy Serum/Plasma Kit (Qiagen) in accordance with the manufacturer's instructions. RNA concentration and purity were detected using a NanoDrop 2000/2000c (Thermo Fisher Scientific, Inc.). In addition, cDNA was prepared from 1 μg RNA using the miScript II RT Kit (Qiagen) following the manufacturer's instructions, and qRT-PCR was conducted using the miScript SYBR® Green PCR kit (Qiagen) following the manufacturer's specifications. U6 served as an internal control for the expression of miR-625-3p in tissues and cell lines. The expression levels of the miR-625-3p in serum were normalized to spiked-in cel-miR-54. The primers for amplification of miR-625-3p (Sangon Biotech, Shanghai, China) were as follows: forward: 5'-GCGCAGGACTATAGAACTTTC-3' and reverse: 5'-GGTCCAGTTTTTTTTTTTTTTTGAG-3'. The qRT-PCR reaction was performed in a Roche Lightcycler 480 Real-Time PCR system (Roche Diagnostics, Basel, Switzerland). The reaction conditions included 95°C for 2 min followed by 40 cycles at 95°C for 10 sec, 55°C for 30 sec, and 72°C for 30 sec. The expression level of miR-625-3p in tissues and cell lines was evaluated by the $2^{-\Delta\Delta CT}$ method, and the relative expression levels of miR-625-3p in serum were determined by $2^{-\Delta CT}$ [22].

Table 4. Sequences of Primers and microRNAs

Primer/microRNA	Sequence
miR-625-3p	Forward: 5'-GCGCAGGACTATAGAACTTTC-3'
	Reverse: 5'-GGTCCAGTTTTTTTTTTTTTTTGAG-3'
U6	Forward: 5'-CTCGCTTCGGCAGCACA-3'
	Reverse: 5'-ACGCTTCACGAATTTGCGT-3'
miR-625-3p mimics	Forward: 5'-GACUAUAGAACUUUCCCCCUCA-3'
	Reverse: 5'-AGGGGGAAAGUUCUAUAGUCUU-3'
miR-625-3p inhibitor	5'-UGAGGGGGAAAGUUCUAUAGUC-3'
NC	Forward: 5'-UUCUCCGAACGUGUCACGUTT-3'
	Reverse: 5'-ACGUGACACGUUCGGAGAATT-3'
inhibitor NC	5'-CAGUACUUUUGUGUAGUACAA-3'

miR, microRNA; NC, negative control; PCR, polymerase chain reaction.

Cell transfection

miR-625-3p mimics, miR-625-3p inhibitor, negative control (NC), or inhibitor negative control (inhibitor NC) were obtained from Genepharma (Shanghai, China). The sequences are listed in **Table 4**. These miRNA mimics, inhibitors, and controls were transfected into Caki-1 and 786-0 cells at a concentration of 50 nM in 6-well plates using Lipofectamine 3000 (Invitrogen) according to the manufacturer's instructions. The cells were harvested for subsequent experiments 48 h after transfection. The transfection efficiency was evaluated by qRT-PCR after 48 h of transfection.

Wound healing assay

The ccRCC cells transfected with miR-625-3p mimics, miR-625-3p inhibitor, NC, or inhibitor NC for 48 h were seeded in 6-well plates containing 3×10^5 cells per well and then incubated to achieve 90-100% confluence. Wounds were created in the confluent cells using a sterile 200-μl pipette tip. After rinsing with phosphate-buffered saline (PBS) three times, cells were cultured in medium without FBS for 24 h at 37°C. Cells were photographed immediately after wounds were created (time 0) and 24 h after wounding. The cell migratory distance was measured after the pictures were acquired.

Cell migration and invasion assay

Transwell chambers with Matrigel (BD Biosciences, Franklin Lakes, NJ, USA) were used for invasion assays, while chambers without Matrigel were used for migration assays. At 48 h after transfection, 3×10^4 transfected cells in 100 μl serum-free medium were seeded in the upper chambers, and 500 μl medium supplemented 10% FBS was added to the bottom of the chambers. Cells were allowed to migrate or invade for 24 or 36 h, respectively. Cells on the upper surface of the chambers were gently scraped. Subsequently, cells on the opposite surface were fixed with 4% paraformaldehyde and stained with 0.1% crystal violet. Pictures of migrated or invaded cells on the opposite surface of the chambers were acquired using a microscope (Leica Microsystems GmbH, Wetzlar, Germany).

Apoptosis assay

Approximately 3×10^5 cells were seeded in 6-well plates and cultured for 24 h to achieve 50% confluent cells. Cells were treated with miR-625-3p mimics, miR-625-3p inhibitor, or the corresponding NC. Then, 48 h after transfection, cells were harvested and washed with cold PBS twice. Cells were re-suspended and labeled with annexin V-fluorescein isothiocyanate/propidium iodide (Invitrogen; Thermo Fisher Scientific, Inc.) for 15 min in the dark according to the manufacturer's instructions. Finally, cell apoptosis was analyzed by flow cytometry (EPICS, XI-4; Beckman Coulter, Inc., Brea, CA, USA).

miRNA target gene prediction and bioinformatics analysis

Target genes of miR-625-3p were predicted using the miRWalk database (http://mirwalk.umm.uni-heidelberg.de/). The clinical information, miRNA sequencing data, and mRNA sequencing data from ccRCC were obtained from TCGA database (https://cancergenome.nih.gov/). The differential expression of mRNAs (DEGs) was analyzed using the edgeR package [23], and only mRNAs with a false-discovery rate (FDR) <0.05 and a |logFC (fold change)|>1 were selected as DEGs. The predicted target genes obtained from miRWalk were matched with the downregulated DEGs. The correlation between target genes and miR-625-3p was measured by Pearson's correlation. A *P*-value <0.05 and an R<-0.2 were considered statistically significant. Survival analysis of target genes was performed according to the clinical information from TCGA, and a P<0.05 was considered statistically significant.

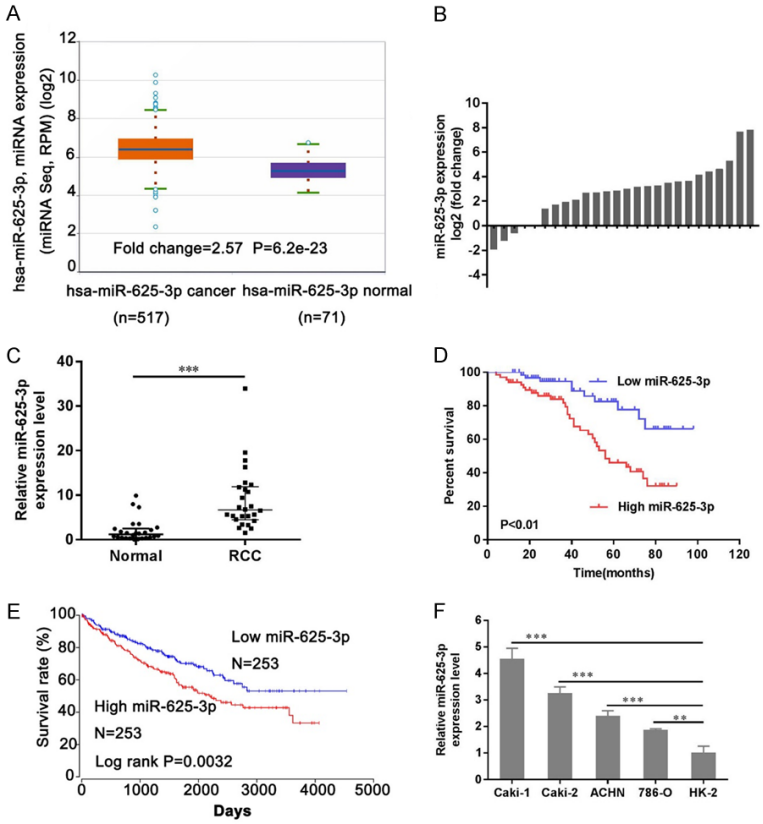

Figure 1. miR-625-3p is upregulated in ccRCC and associate with poor prognosis of ccRCC patients. A. starBase v3.0 indicated miR-625-3p is upregulated in ccRCC compared with normal renal tissues. B. miR-625-3p expression in 30 pairs of ccRCC tissues and the adjacent normal renal tissues. C. Scatter plots illustrating RT-qPCR analysis of expression fold change for miR-625-3p in ccRCC tissues compared with matched adjacent normal renal tissues. miR-625-3p was upregulated in ccRCC tissues compared with adjacent normal renal tissues. D, E. The Kaplan-Meier curves with univariate analyses of overall survival inO our study and TCGA database suggested that patients with high miR-625-3p expression hasve poorer overall survival rates than patients with low miR-625-3p expression. F. miR-625-3p is upregulated in ccRCC cells compared to HK-2. *P<0.05, **P<0.01, ***P<0.001.

Statistical analysis

Statistical analysis was performed using SPSS 19.0 (IBM Corp., Armonk, NY, USA) or GraphPad Prism version 7.0 (GraphPad Software Inc., San Diego, CA, USA). The Pearson χ^2 test was used to assess the statistical significance of the association between the expression of miR-625-3p and the patient's clinicopathological parameters. Comparisons between groups were performed using the Student's *t*-test or a one-way ANOVA Dunnett's post-hoc test. Calculated *P*-values of <0.05 were considered statistically significant. The data are shown as means ± standard deviation (SD). Setting the median as a cutoff point, the expression level of miR-625-3p was classified into high and low groups. Survival analysis was performed using the log-rank test and Cox regression analyses. Receiver-operating characteristic (ROC) curves and the area under the ROC curve (AUC) were used to evaluate the diagnostic values of miR-625-3p for the diagnosis of ccRCC. Resulting *P*-values of <0.05 were considered statistically significant.

Results

miR-625-3p is highly expressed in ccRCC tissues and ccRCC cells

According to analysis of the TCGA dataset using starBase v3.0, miR-625-3p is upregulated in ccRCC (**Figure 1A**). Thus, we performed real-time PCR on 30 pairs of ccRCC tissues and adjacent normal renal tissues. A total of 83.3% (25 of 30) of the ccRCC samples exhibited at least a 2-fold increase in expression of miR-625-3p compared with their corresponding normal renal tissues (**Figure 1B**). The median miR-625-3p expression in ccRCC tissues was significantly higher than that in normal renal tissues (P<0.001, **Figure 1C**). We also examined miR-625-3p expression in 136 FFPE ccRCC tissues and analyzed the correlation between miR-625-3p expression and clinicopathological parameters in these samples. We identified a statistically significant increase in expression of miR-625-3p in late stages (stages III and IV) of ccRCC compared with early stage (stages I and II; P<0.05; **Table 2**). In addition, we failed to uncover a statistically significant difference in miR-625-3p expression level according to gender, age, or tumor size (**Table 2**). Subsequently, Cox regression analysis was conducted at both the univariate and multivariate level. In the uni-

Table 5. miR-625-3p expression and patients' survival

Variable	Overall Survival	
	HR[1] (95% CI[2])	*P* value
Univariate analysis		
miR-625-3p		
Low	1	
High	3.080 (1.505-6.305)	0.002
Age	0.656 (0.342-1.256)	0.203
Sex	1.004 (0.508-1.985)	0.991
Tumor Size	1.337 (0.710-2.518)	0.369
Tumor Stage	2.453 (1.315-4.576)	0.005
Multivariate analysis[3]		
miR-625-3p		
Low	1	
High	2.949 (1.413-6.152)	0.004
Age	0.848 (0.431-1.670)	0.634
Sex	1.274 (0.623-2.604)	0.507
Tumor Size	1.581 (0.804-3.111)	0.185
Tumor Stage	2.036 (1.063-3.901)	0.032

[1]Hazard ratio, estimated from Cox proportional hazard regression model. [2]Confidence interval of the estimated HR. [3]Adjusted for patients' age, gender, tumor stage, and tumor size.

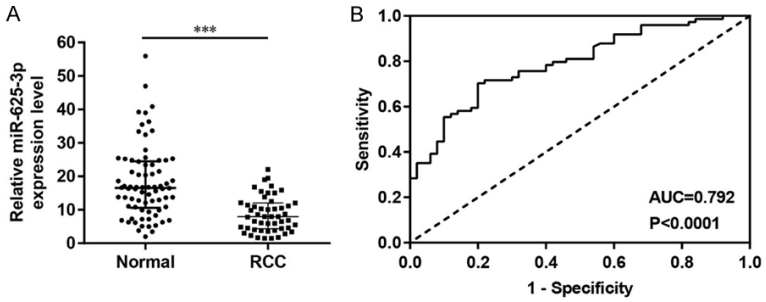

Figure 2. Diagnostic value of miR-625-3p in ccRCC. A. miR-625-3p was down-regulated in serum from ccRCC patients compared to that from healthy controls. B. The ROC analysis for detection of ccRCC patients from health controls using miR-625-3p. ***P<0.001.

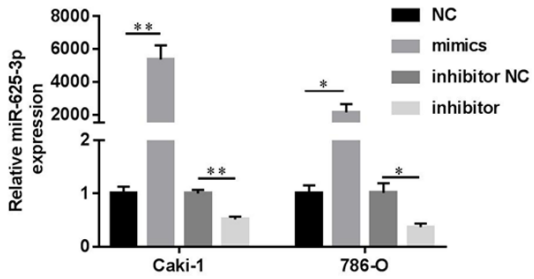

Figure 3. miR-625-3p expression in Caki-1 and 786-O was significantly upregulated after transfection with miR-625-3p mimics but downregulated after transfection with miR-625-3p inhibitor compared with that transfected with corresponding negative control. *P<0.05, **P<0.01, ***P<0.001.

variate analysis, patients with high miR-625-3p expression based on a median cutoff showed a significantly shorter overall survival (hazard ratio [HR]=3.080; 95% confidence intervals [CI]=1.505-6.305; P=0.002) compared to those with low miR-625-3p expression (**Table 5**). In the multivariate analysis, patients with high miR-625-3p again had shorter overall survival compared with those with low miR-625-3p (HR=2.949; 95% CI=1.413-6.152; P=0.004; **Table 5**). Furthermore, Kaplan-Meier analysis illustrated that patients with high miR-625-3p demonstrate lower overall survival rates than those with low miR-625-3p levels (**Figure 1D**), consistent with the results from TCGA database analysis (**Figure 1E**).

Additionally, the expression level of miR-625-3p was measured in ccRCC cell lines and HK-2. In agreement with patient sample results, miR-625-3p expression in ccRCC cell lines was significantly higher than that in HK-2 cells (P< 0.01, **Figure 1F**). Among these ccRCC cell lines, Caki-1 exhibited the highest miR-625-3p expression, while 786-O cells exhibited the lowest miR-625-3p expression. Thus, these two cell lines were selected for further analysis via in vitro assays.

Diagnostic value of the miR-625-3p in ccRCC

Real-time PCR was performed on 50 ccRCC patients and 74 HCs. Serum miR-625-3p level was significantly lower in ccRCC patients than in HCs (P<0.001; **Figure 2A**). ROC curve analysis indicated that the serum miR-625-3p level might serve as a useful biomarker for differentiating patients with ccRCC from those with HCs; the AUC was 0.792 (95% CI, 0.714-0.870) and the sensitivity and specificity was 70.3 and 80.0%, respectively (**Figure 2B**).

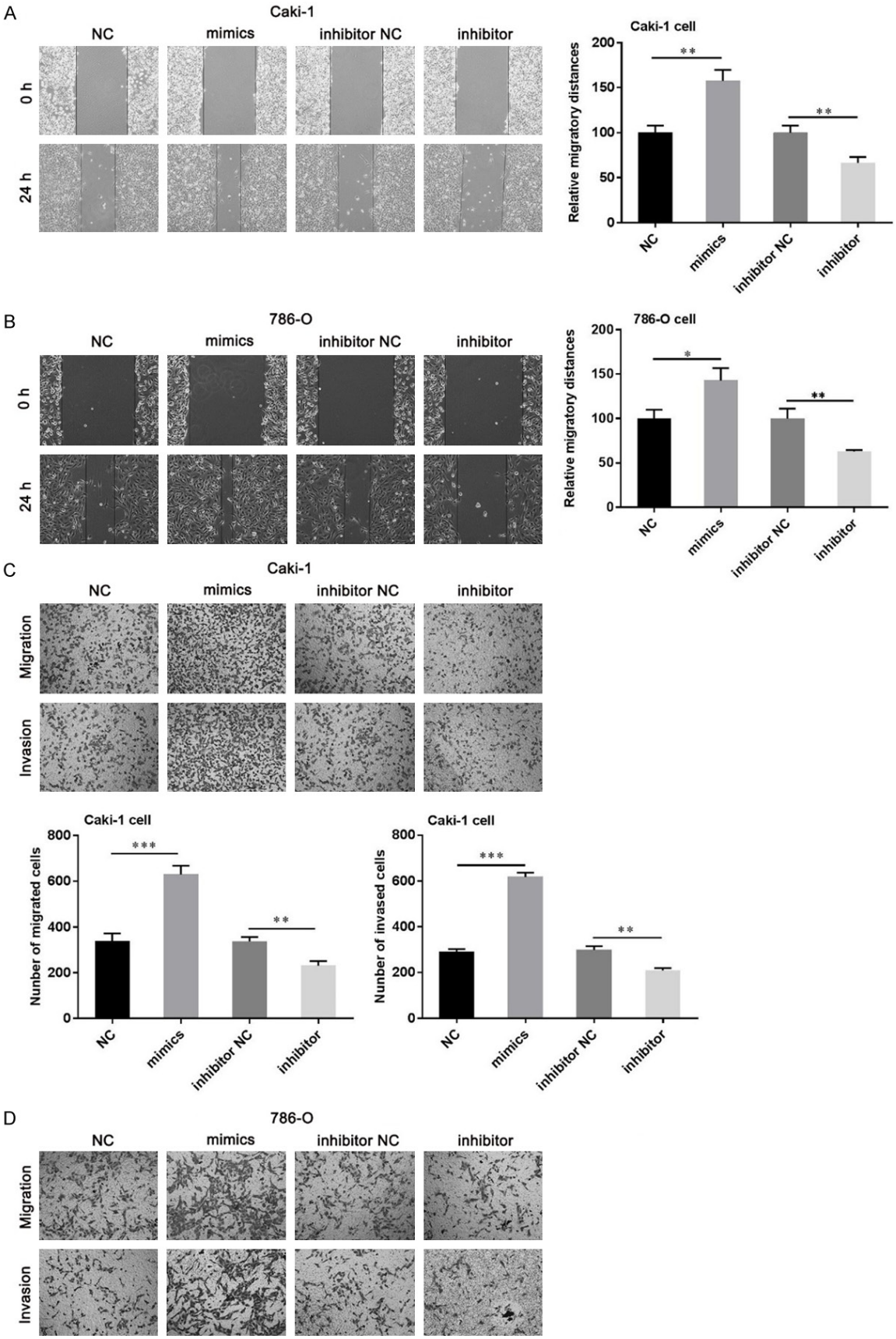
A
Caki-1
NC
mimics
inhibitor NC
inhibitor
0 h
24 h
Caki-1 cell
Relative migratory distances
200
150
100
50
0
**
**
NC
mimics
inhibitor NC
inhibitor
B
786-O
NC
mimics
inhibitor NC
inhibitor
0 h
24 h
786-O cell
Relative migratory distances
200
150
100
50
0
*
**
NC
mimics
inhibitor NC
inhibitor
C
Caki-1
NC
mimics
inhibitor NC
inhibitor
Migration
Invasion
Caki-1 cell
Nunber of migrated cells
800
600
400
200
0
***
**
NC
mimics
inhibitor NC
inhibitor
Caki-1 cell
Nunber of invased cells
800
600
400
200
0
***
**
NC
mimics
inhibitor NC
inhibitor
D
786-O
NC
mimics
inhibitor NC
inhibitor
Migration
Invasion

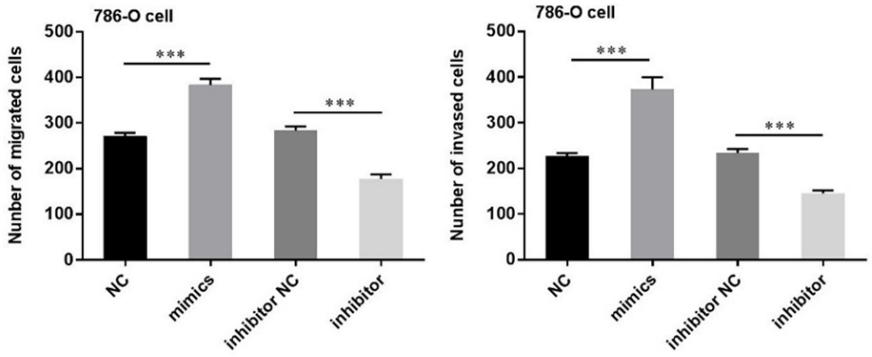

Figure 4. miR-625-3p accelerate ccRCC cells migration and invasion. A. Wound healing assay was used to evaluate the motility of ccRCC cell lines. The migratory distance was measured and compared at 24 hours later. Wound healing assay showed that overexpression of miR-625-3p promoted Caki-1 cells migration, and inhibition of miR-625-3p attenuated Caki-1 cells migration. B. Wound healing assay showed that overexpression of miR-625-3p promoted 786-O cells migration, and inhibition of miR-625-3p attenuated 786-O cells migration. C. Transwell assays indicated the migration and invasion capability of ccRCC cell lines. Twenty-four hours later, these cells passed though the membrane were calculated and compared. Transwell assay revealed that overexpression of miR-625-3p promoted Caki-1 cells migration and invasion, and inhibition of miR-625-3p reduced Caki-1 cells migration and invasion. D. Transwell assay revealed that overexpression of miR-625-3p promoted 786-O cells migration and invasion, and inhibition of miR-625-3p reduced 786-O cells migration and invasion. $^{*}P<0.05$, $^{**}P<0.01$, $^{***}P<0.001$.

miR-625-3p promotes migration and invasion of ccRCC cells

To further elucidate the role of miR-625-3p in ccRCC development, Caki-1 and 786-O cells were transfected with miR-625-3p mimics, inhibitor, or NCs. Then, qRT-PCR was used to detect the transfection efficiency. miR-625-3p expression in Caki-1 and 786-O was significantly upregulated after transfection with miR-625-3p mimics but downregulated after transfection with miR-625-3p inhibitor compared with that transfected with corresponding negative control (**Figure 3**). A wound healing assay was performed to detect the migration ability of 786-O and Caki-1 cells. Overexpression of miR-625-3p markedly enhanced the cell migration of 786-O and Caki-1 cells compared to that of cells transfected with NC, while inhibition of miR-625-3p markedly attenuated the cell migration of 786-O and Caki-1 cells compared to that of cells transfected with inhibitor NC (**Figure 4A**, **4B**). Moreover, overexpression of miR-625-3p significantly enhanced both cell migration and invasion of Caki-1 cells compared to levels in cells transfected with NC. As expected, inhibition of miR-625-3p markedly attenuated both the cell migration and invasion of Caki-1 cells compared to levels in cells transfected with inhibitor NC (**Figure 4C**). Similar results were observed in 786-O cells (**Figure 4D**). In summation, these findings revealed that miR-625-3p promotes the migration and invasion of ccRCC cells in vitro.

miR-625-3p suppresses apoptosis of ccRCC cells

We next investigated the function of miR-625-3p on ccRCC cell apoptosis. Flow cytometry analysis of apoptosis in ccRCC cells indicated that overexpression of miR-625-3p reduced apoptosis in Caki-1 cells compared to levels in cells transfected with NC. Additionally, inhibition of miR-625-3p promoted the apoptosis of Caki-1 cells compared to levels in cells transfected with inhibitor NC. Similar results were obtained with 786-O cells (**Figure 5**). These data demonstrate that miR-625-3p promotes apoptosis of ccRCC cells in vitro.

Prediction of miR-625-3p target genes associated with ccRCC

Based on the fact that miRNAs exert their effects via regulation of target gene expression by binding to the 3'-UTR of mRNA [8], we sought to identify miR-625-3p target genes involved in ccRCC. Using miRWalk, a total of 951 predicted targets of miR-625-3p were identified. According to the TCGA database, a total of 5212 DEGs were identified, and 2354 DEGs were downregulated. Importantly, we found nine genes (ANK3, TLN2, CLCN5, CHDH, FREM2,

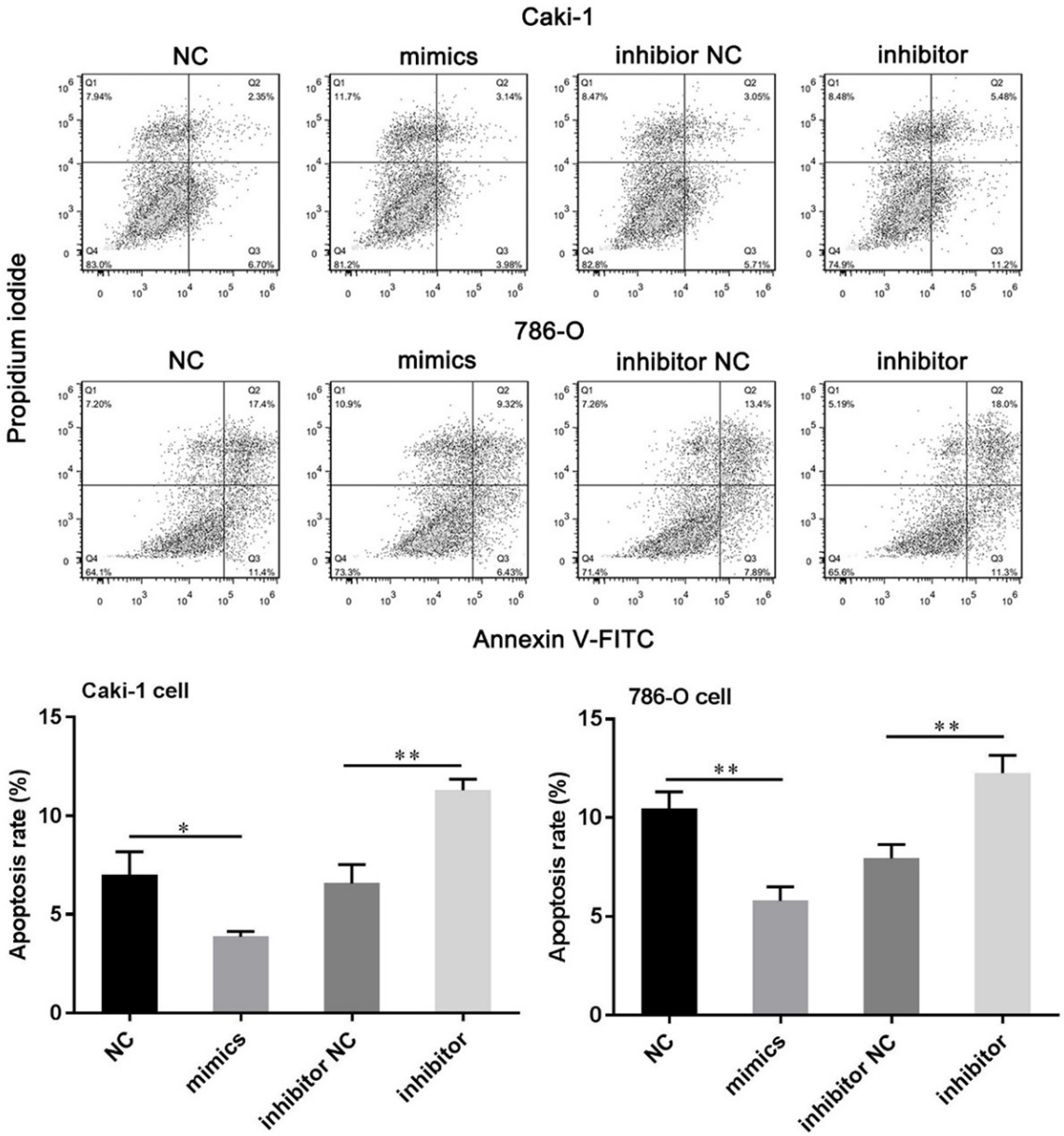

Figure 5. Flow cytometric apoptosis assay determined that miR-625-3p repressed ccRCC cells apoptosis. Overexpression of miR-625-3p suppressed the apoptosis ability of Caki-1 cells compared with cells transfected with NC. Knockdown of miR-625-3p enhanced the apoptosis ability of 786-O cells compared with cells transfected with inhibitor NC. *P<0.05, **P<0.01, ***P<0.001. Q3 represents the apoptosis rate.

THRB, EPB41L5, NEBL and PLCL1) that were negatively correlated with miR-625-3p expression (**Table 6**). In addition, all nine of these genes were associated with a lower overall survival of ccRCC patients (**Table 7**).

Discussion

In this study, we demonstrated that miR-625-3p is upregulated in ccRCC tissues and that increased miR-625-3p is positively correlated with lower overall survival in ccRCC patients. However, miR-625-3p was down-regulated in serum of ccRCC patients. And miR-625-3p could serve as a prognostic biomarker. Subsequent in vitro functional studies indicated that miR-625-3p promotes ccRCC cell migration and invasion and suppresses apoptosis of ccRCC cells.

Previous studies indicated that abnormal expression of miR-625-3p plays a critical role in

Table 6. Target genes of miR-625-3p predicted by miRWalk

Gene	R	*P*-value
ANK3	-0.215	<0.001
TLN2	-0.219	<0.001
CLCN5	-0.259	<0.001
CHDH	-0.222	<0.001
FREM2	-0.271	<0.001
THRB	-0.264	<0.001
EPB41L5	-0.247	<0.001
NEBL	-0.247	<0.001
PLCL1	-0.288	<0.001

R, coefficient of correlation.

Table 7. The survival analysis of genes by data from TCGA database

Gene	HR (95% CI)	*P*-value
ANK3	0.920 (0.894-0.946)	<0.001
TLN2	0.949 (0.933-0.967)	<0.001
CLCN5	0.971 (0.961-0.982)	<0.001
CHDH	0.966 (0.953-0.978)	<0.001
FREM2	0.896 (0.857-0.936)	<0.001
THRB	0.852 (0.798-0.911)	<0.001
EPB41L5	0.929 (0.901-0.958)	<0.001
NEBL	0.957 (0.939-0.974)	<0.001
PLCL1	0.917 (0.883-0.952)	<0.001

several cancers, including oral squamous cell carcinoma [19], colorectal carcinoma [24], and thyroid cancer [20]. In colorectal cancer, miR-625-3p is upregulated and promotes cell migration and invasion by targeting SCAI [24]. Furthermore, high expression of miR-625-3p was reported to be associated with the resistance of colorectal cancer to oxaliplatin treatment [25, 26]. In thyroid cancer, miR-625-3p promotes the proliferation, migration, and invasion of cancer cells by targeting AEG-1 [20]. Xu and colleagues reported that miR-625-3p promotes oral squamous cell carcinoma migration via inhibition of SCAI [27]. Furthermore, Kirschner and colleagues demonstrated that increased miR-625-3p in plasma may serve as a potential biomarker for patients with malignant pleural mesothelioma [28]. These studies suggest that miR-625-3p can serve as an oncogene or tumor suppressor in cancers.

In this study, we found that miR-625-3p was upregulated in ccRCC and that 83.3% of the ccRCC patient samples displayed ≥2-fold increase in expression of miR-625-3p compared with their corresponding healthy adjacent renal tissues. In addition, we found that high expression of miR-625-3p is associated with poor overall survival in ccRCC patients, and additional functional assays identified a role of miR-625-3p in ccRCC via effects on migration, invasion, and apoptosis of ccRCC cells. The underlying mechanism of miR-625-3p regulation of ccRCC progression, however, remains unclear, and animal experiments are necessary to further elucidate the function of miR-625-3p in vivo.

Interestingly, in this study, we found that the expression of miR-625-3p is inconsistent in ccRCC tissues and serum. The expression of miR-625-3p was increased in ccRCC tissues than that of normal renal tissues, however, miR-625-3p was decreased in serum of ccRCC patients than that of healthy controls. This phenomenon can be explained by the mechanism of selective release of miRNA from tumor cells into body fluids such as blood [29]. Ostenfeld and colleagues identified that selective secretion of tumor-suppressor miRNA was associated with bladder cancer metastasis [30]. Thus, miR-625-3p retained in tumor tissues might contribute to the ccRCC malignant phenotype transition.

In conclusion, we demonstrated that overexpression of miR-625-3p promotes the migration and invasion of ccRCC cells and reduces the apoptosis of these cells. Furthermore, high expression of miR-625-3p was associated with an unfavorable prognosis for ccRCC patients. In addition, miR-625-3p could be used as biomarkers for discriminating ccRCC patients from healthy individuals. Therefore, our results suggest that miR-625-3p may serve as a novel biomarker for survival and non-invasive diagnosis of ccRCC patients and offer a potential therapeutic target for treating these patients.

Acknowledgements

This study was supported by Basic Research Project of Peking University Shenzhen Hospital (JCYJ2017001, JCYJ2017004, JCYJ20170-05, JCYJ2017006, JCYJ2017007, JCYJ20170-12), Clinical Research Project of Peking University Shenzhen Hospital (LCYJ2017001), Science and Technology Development Fund Project of Shenzhen (no. JCYJ20170307111334308)

and Clinical Research Project of Shenzhen Health Commission (no. SZLY2018023).

Disclosure of conflict of interest

None.

Address correspondence to: Yongqing Lai, Guangdong and Shenzhen Key Laboratory of Male Reproductive Medicine and Genetics, Peking University Shenzhen Hospital, Clinical College of Anhui Medical University, 1120 Lianhua Road, Shenzhen 518036, Guangdong, P. R. China. Tel: 86-0755-83923333-2731, E-mail: yqlord@163.com

References

[1] Siegel RL, Miller KD and Jemal A. Cancer statistics, 2018. CA Cancer J Clin 2018; 68: 7-30.
[2] Hsieh JJ, Purdue MP, Signoretti S, Swanton C, Albiges L, Schmidinger M, Heng DY, Larkin J and Ficarra V. Renal cell carcinoma. Nat Rev Dis Primers 2017; 3: 17009.
[3] Rossi SH, Klatte T, Usher-Smith J and Stewart GD. Epidemiology and screening for renal cancer. World J Urol 2018.
[4] Nabi S, Kessler ER, Bernard B, Flaig TW and Lam ET. Renal cell carcinoma: a review of biology and pathophysiology. F1000Res 2018; 7: 307.
[5] Massari F, Di Nunno V, Ciccarese C, Graham J, Porta C, Comito F, Cubelli M, Iacovelli R and Heng DYC. Adjuvant therapy in renal cell carcinoma. Cancer Treat Rev 2017; 60: 152-157.
[6] Barata PC and Rini BI. Treatment of renal cell carcinoma: current status and future directions. CA Cancer J Clin 2017; 67: 507-524.
[7] Diaz de Leon A and Pedrosa I. Imaging and screening of kidney cancer. Radiol Clin North Am 2017; 55: 1235-1250.
[8] Chen G, Lu L, Liu C, Shan L and Yuan D. MicroRNA-377 suppresses cell proliferation and invasion by inhibiting TIAM1 expression in hepatocellular carcinoma. PLoS One 2015; 10: e0117714.
[9] Fang L, Deng Z, Shatseva T, Yang J, Peng C, Du WW, Yee AJ, Ang LC, He C, Shan SW and Yang BB. MicroRNA miR-93 promotes tumor growth and angiogenesis by targeting integrin-beta8. Oncogene 2011; 30: 806-821.
[10] Sun X, Dai G, Yu L, Hu Q, Chen J and Guo W. miR-143-3p inhibits the proliferation, migration and invasion in osteosarcoma by targeting FOSL2. Sci Rep 2018; 8: 606.
[11] Jia YJ, Liu ZB, Wang WG, Sun CB, Wei P, Yang YL, You MJ, Yu BH, Li XQ and Zhou XY. HDAC6 regulates microRNA-27b that suppresses proliferation, promotes apoptosis and target MET in diffuse large B-cell lymphoma. Leukemia 2018; 32: 703-711.
[12] Fan Y, Ma X, Li H, Gao Y, Huang Q, Zhang Y, Bao X, Du Q, Luo G, Liu K, Meng Q, Zhao C and Zhang X. miR-122 promotes metastasis of clear-cell renal cell carcinoma by downregulating Dicer. Int J Cancer 2018; 142: 547-560.
[13] Kabir TD, Ganda C, Brown RM, Beveridge DJ, Richardson KL, Chaturvedi V, Candy P, Epis M, Wintle L, Kalinowski F, Kopp C, Stuart LM, Yeoh GC, George J and Leedman PJ. A microRNA-7/growth arrest specific 6/TYRO3 axis regulates the growth and invasiveness of sorafenib-resistant cells in human hepatocellular carcinoma. Hepatology 2018; 67: 216-231.
[14] Chen X, Wang X, Ruan A, Han W, Zhao Y, Lu X, Xiao P, Shi H, Wang R, Chen L, Chen S, Du Q, Yang H and Zhang X. miR-141 is a key regulator of renal cell carcinoma proliferation and metastasis by controlling EphA2 expression. Clin Cancer Res 2014; 20: 2617-2630.
[15] Zhai W, Ma J, Zhu R, Xu C, Zhang J, Chen Y, Chen Z, Gong D, Zheng J, Chen C, Li S, Li B, Huang Y, Xue W and Zheng J. MiR-532-5p suppresses renal cancer cell proliferation by disrupting the ETS1-mediated positive feedback loop with the KRAS-NAP1L1/P-ERK axis. Br J Cancer 2018; 119: 591-604.
[16] Xiao H, Xiao W, Cao J, Li H, Guan W, Guo X, Chen K, Zheng T, Ye Z, Wang J and Xu H. miR-206 functions as a novel cell cycle regulator and tumor suppressor in clear-cell renal cell carcinoma. Cancer Lett 2016; 374: 107-116.
[17] Xu X, Wu J, Li S, Hu Z, Xu X, Zhu Y, Liang Z, Wang X, Lin Y, Mao Y, Chen H, Luo J, Liu B, Zheng X and Xie L. Downregulation of microRNA-182-5p contributes to renal cell carcinoma proliferation via activating the AKT/FOXO3a signaling pathway. Mol Cancer 2014; 13: 109.
[18] Jingushi K, Ueda Y, Kitae K, Hase H, Egawa H, Ohshio I, Kawakami R, Kashiwagi Y, Tsukada Y, Kobayashi T, Nakata W, Fujita K, Uemura M, Nonomura N and Tsujikawa K. miR-629 targets TRIM33 to promote TGFbeta/Smad signaling and metastatic phenotypes in ccRCC. Mol Cancer Res 2015; 13: 565-574.
[19] Xu D, Gu M and Liu HL. MicroRNA-625-3p promotes cell migration of oral squamous cell carcinoma by regulating SCAI expression. Eur Rev Med Pharmacol Sci 2019; 23: 641-648.
[20] Fang L, Kong D and Xu W. MicroRNA-625-3p promotes the proliferation, migration and invasion of thyroid cancer cells by up-regulating astrocyte elevated gene 1. Biomed Pharmacother 2018; 102: 203-211.
[21] Jiang Q, Lu X, Huang P, Gao C, Zhao X, Xing T, Li G, Bao S and Zheng H. Expression of miR-652-3p and effect on apoptosis and drug sensitivity in pediatric acute lymphoblastic leukemia. Biomed Res Int 2018; 2018: 5724686.

[22] Livak KJ and Schmittgen TD. Analysis of relative gene expression data using real-time quantitative PCR and the 2(-Delta Delta C(T)) Method. Methods 2001; 25: 402-408.
[23] Robinson MD, McCarthy DJ and Smyth GK. edgeR: a Bioconductor package for differential expression analysis of digital gene expression data. Bioinformatics 2010; 26: 139-140.
[24] Zheng H, Ma R, Wang Q, Zhang P, Li D, Wang Q, Wang J, Li H, Liu H and Wang Z. MiR-625-3p promotes cell migration and invasion via inhibition of SCAI in colorectal carcinoma cells. Oncotarget 2015; 6: 27805-27815.
[25] Rasmussen MH, Lyskjaer I, Jersie-Christensen RR, Tarpgaard LS, Primdal-Bengtson B, Nielsen MM, Pedersen JS, Hansen TP, Hansen F, Olsen JV, Pfeiffer P, Orntoft TF and Andersen CL. miR-625-3p regulates oxaliplatin resistance by targeting MAP2K6-p38 signalling in human colorectal adenocarcinoma cells. Nat Commun 2016; 7: 12436.
[26] Rasmussen MH, Jensen NF, Tarpgaard LS, Qvortrup C, Romer MU, Stenvang J, Hansen TP, Christensen LL, Lindebjerg J, Hansen F, Jensen BV, Hansen TF, Pfeiffer P, Brunner N, Orntoft TF and Andersen CL. High expression of microRNA-625-3p is associated with poor response to first-line oxaliplatin based treatment of metastatic colorectal cancer. Mol Oncol 2013; 7: 637-646.
[27] Li Y, Tao C, Dai L, Cui C, Chen C, Wu H, Wei Q and Zhou X. MicroRNA-625 inhibits cell invasion and epithelial-mesenchymal transition by targeting SOX4 in laryngeal squamous cell carcinoma. Biosci Rep 2019; 39.
[28] Kirschner MB, Cheng YY, Badrian B, Kao SC, Creaney J, Edelman JJ, Armstrong NJ, Vallely MP, Musk AW, Robinson BW, McCaughan BC, Klebe S, Mutsaers SE, Zandwijk N and Reid G. Increased circulating miR-625-3p: a potential biomarker for patients with malignant pleural mesothelioma. J Thorac Oncol 2012; 7: 1184-1191.
[29] Pigati L, Yaddanapudi SC, Iyengar R, Kim DJ, Hearn SA, Danforth D, Hastings ML and Duelli DM. Selective release of microRNA species from normal and malignant mammary epithelial cells. PLoS One 2010; 5: e13515.
[30] Ostenfeld MS, Jeppesen DK, Laurberg JR, Boysen AT, Bramsen JB, Primdal-Bengtson B, Hendrix A, Lamy P, Dagnaes-Hansen F, Rasmussen MH, Bui KH, Fristrup N, Christensen EI, Nordentoft I, Morth JP, Jensen JB, Pedersen JS, Beck M, Theodorescu D, Borre M, Howard KA, Dyrskjot L and Orntoft TF. Cellular disposal of miR23b by RAB27-dependent exosome release is linked to acquisition of metastatic properties. Cancer Res 2014; 74: 5758-5771.